

Kinetics, equilibrium, and thermodynamic studies of sulphate adsorption from aqueous solution using activated carbon derived from rice straw

E. Farahmand^{1*}, B. Rezai², F. Doulati Ardejani³, S.Z. Shafaei Tonekaboni³

¹Department of Mining Engineering, Science and Research Branch, Islamic Azad University, Tehran, Iran

²Department of Mining and Metallurgical Engineering, Amirkabir University, Tehran, Iran.

³School of Mining, College of Engineering, University of Tehran, Tehran, Iran

Received June 26, 2015, Revised September 10, 2015

In this study, the possibility of sulphate adsorption from a synthetic solution containing sodium sulphate was investigated using activated carbon derived from rice straw by $ZnCl_2$ activation. The structural and morphological characteristics of rice straw and activated carbon were evaluated applying SEM, FTIR, and EDS techniques. Influence of various parameters such as agitation time, pH, temperature, sulphate concentration and adsorbent dose at 5 levels was also studied. The highest uptake of sulphate ions was determined as 56.49 mg/g (1.8 mg/g compared to adsorption by raw straw). Adsorption kinetics and sulphate adsorption equilibrium behaviour were studied. It was found that the adsorption process follows second-order kinetics model and Langmuir isotherm fits well the equilibrium data. ΔG^0 was found to be -3.208, -3.230, -3.317, -3.372, -3.427 and -3.482 KJ/mol at 20, 25, 30, 35, 40, and 45°C, respectively. ΔS^0 and ΔH^0 of the adsorption were 10.95 J/K/mol and 0.001076 KJ/mol, respectively. The results further show that the adsorption process was a spontaneous and endothermic reaction and the activated carbon derived from rice straw by $ZnCl_2$ chemical activation can be considered as an effective adsorbent for sulphate adsorption from the aqueous solutions.

Key words: Adsorption; Activated Carbon; Sulphate; Isotherm; Adsorption Kinetic; $ZnCl_2$ activation.

INTRODUCTION

Pollutants release, generation of the variety of organic and inorganic chemical compounds due to the rapid development of chemical industry, and entry of toxic and hazardous substances to natural resources have become a serious threat to environment. Analysis of the effluents from mining industry has shown that this type of waste is considered among the most dangerous industrial waste. Besides, they contain high concentrations of toxic elements due to high levels of the variety of minerals. The annual costs which are paid for the treatment of such polluted effluents are considerable [1]. Sulphate ion is one of the major oxidation products of sulphide minerals in the tailings of ore processing plant and low-grade waste dumps containing sulphide minerals. Rapid oxidation of sulphide minerals in particular pyrite in the presence of oxygen and moisture produces acid mine drainage (AMD). Acid mine drainage results in death of vegetation, death of aquatic life, surface and groundwater pollution and corrosion of mine equipment [2]. Common methods of removing toxic elements from the the industrial effluents include precipitation, coagulation, ion exchange, electro-dialysis, electro-conglutination,

reverse osmosis, evaporation, and filtration [3, 4]. Although there are several techniques for removing dangerous elements from the aqueous solutions, most processes have significant disadvantages such as need for high energy and costly process, low efficiency, production of high amounts of sludge, sludge disposal problems, high levels of trace elements, high cost of specialty chemicals, and reclamation processes [3, 5]. Therefore, due to technical and economic constraints of the previous methods, the search for new methods is recommended and, in this regard, the biological uptake as a new option has been considered [6]. Biological adsorption or biosorption, is the process of using biological materials such as bacteria, fungi, algae, and agricultural waste through the creation of complex to toxic elements. Biological adsorption mechanism involves in chemical bonding between the metal ions and adsorbent surface groups or ion exchange reaction due to high ion exchange capacity of the adsorbent. Since this process is low-cost, and eco-friendly as well as having high performance in adsorption, it is an efficient alternative to the traditional methods in terms of removal of toxic elements [7]. Thus, in recent years, the use of agricultural byproducts and residuals like bark, sawdust, pistachio skin, almond skin, rice and wheat bran, corn residue, etc. due to the presence of cellulose compounds, carbon, and

To whom all correspondence should be sent:
E-mail: Farahmand.ehsan@yahoo.com

silica in their chemical structures has highly increased to adsorb toxic elements from the water and wastewater [8]. These biological materials are overabundant and available. However, they are not used specifically. Activated carbon as an adsorbent with high adsorption capacity has many applications in adsorption processes of liquid or gas phase. Activated carbon could be produced using both physical and chemical methods [9, 10]. The purpose of activation is the creation of porous structure with a high free surface area in raw materials [11]. In this study, rice straw is used by chemical activation to produce activated carbon.

EXPERIMENTAL PROCEDURE

Material and methods

Chemicals used in this study included sodium sulphate from Merck, deionised water to prepare the solution containing sulphate, hydrochloric acid and ammonia for pH adjustment from Merck, zinc chloride with the purity of 98 to 100 percent as well as molar mass of 136.28 g/mol, and distilled water to dilute solution system. Rice straw used in this research was prepared from the agricultural lands in Mazandaran Province in the north of Iran. In order to prepare the adsorbent, the rice straw was minced in an electric mill; then, it was washed several times with double distilled water and the oven was kept at 60°C to dry the adsorbent completely.

Raw material was mixed with ZnCl₂ boiling solution to combine them in a 2: 1 ratio and, the mixture was put on the heater at 100°C in order to evaporate the moisture. It was then put in the oven for 4 h at 150°C when completely dried. The resulting material was placed in a vacuum furnace for 1 h at 500°C. The adsorbent obtained was washed with the distilled water and then dried in the oven at 100°C. The obtained activated carbon was screened to reach the size of 250-500 μ using ASTM E11, 45 mesh sieve. Scanning electronic microscope (SEM) shows a layer of raw straw and activated carbon, as presented in Fig. 1. In addition, Fig. 2 demonstrate the functional groups and their links as well as their areas for raw straw and activated carbon using Fourier transform infrared spectroscopy (FTIR). The broader adsorption peak around 3440 cm⁻¹ could be attributed to the stretching of H-bonded hydroxyl groups. The other adsorption at 2914 cm⁻¹ relates to the C-H stretching. The band at 1649.15 cm⁻¹ is assigned to the bending mode of the adsorbed water [12]. In contrast to raw rice straw, there is a sharp adsorption peak of the stretching vibration of C-N

bond at 603.68 cm⁻¹ in ZnCl₂ activated rice straw carbon.

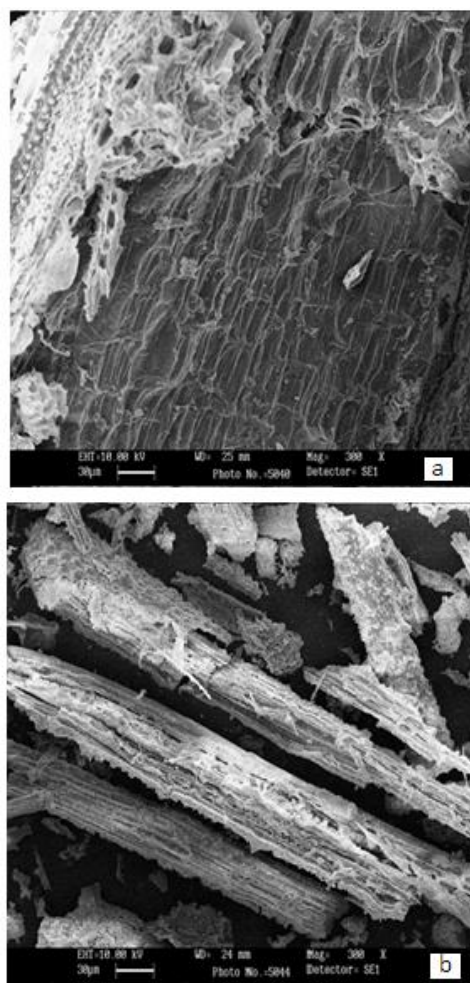


Fig. 1. SEM images of raw straw (a) and activated carbon mixed with ZnCl₂ (b).

Adsorption studies

Adsorption experiments were carried out in a batch system to determine solution pH, equilibrium time, optimum temperature, adsorbent dose, adsorption capacity, as well as the optimal kinetics and isotherm models and calculate the thermodynamic parameters. In this study, during the reaction time, a mixture of the certain amount of adsorbent and 30 mL solution containing a definite concentration of sulphate were placed on a thermostated rotary shaker for stirring intensity at 200 rpm and, after each experiment, the amount of remaining sulphate in the solution was measured and the amount of sulphate uptake was determined in each experiment. After completing the reaction, the amount of adsorbed sulphate was determined by calculating the difference between the initial and final concentrations and the quantity of adsorbed sulphate ions was calculated by the following equation:

$$q_e = \frac{(C_0 - C_e)v}{m}, \quad (1)$$

where q_e is the amount of adsorbed sulphate (mg/g), C_0 and C_e represent the initial and equilibrium concentrations of sulphate (mg/L), m denotes mass of adsorbent (g), and v stands for the volume of the solution (L).

In this study, influence of various parameters such as contact time, pH, temperature, sulphate concentration, and adsorbent dose using experimental design at five levels has been studied.

The optimization study of sulphate adsorption are presented in Table 1.

Effect of temperature

Temperature change is an important factor in determining the adsorption capacity. Effect of temperature on sulphate adsorption was studied at 20, 25, 30, 35, 40, and 45°C in the thermostated rotary shaker and the results show that the uptake slightly increased linearly with the temperature. It remained constant at temperatures above 25°C. Studies reveal that this increase is related to the increased temperature, the number of active sites,

and adsorption rate. Besides, at higher temperatures, the adsorption of sulphate might be decreased due to the damage and destruction of the active sites [13,19]. Fig. 3 shows the effect of temperature on the sulphate adsorption process.

Effect of contact time

Contact time is one of the effective factors in bioadsorption study. It plays an important role in improving the adsorption reaction and leads the reaction to the equilibrium. As shown in Fig. 4, during the first few minutes of the process, the adsorption rate increased intensely. It increased again with a gradual rate. The adsorption reached the maximum value after 90 min. After that, the adsorption remained constant with time [13]. The reason is that at the beginning of the adsorption reaction the number of sites available for adsorption is high. This results in high adsorption. The remaining sites are filled due to the repulsive force between sulphate ions in the liquid phase and activated carbon in solid phase. As a result, the amount of adsorption is reduced gradually.

Table 1. Values of sulphate adsorption parameters of 5 levels.

Exam Number	Time (min)	pH	Temperature (°C)	Concentration (mg/L)	Adsorbent dose (g)	Uptake (mg/g)
1	5	2	20	250	0.02	51
2	5	3	25	350	0.04	5.25
3	5	4	30	450	0.06	10
4	5	5	35	550	0.08	8.3
5	5	6	40	650	0.1	6.9
6	10	2	25	450	0.08	6.37
7	10	3	30	550	0.1	8.4
8	10	4	35	650	0.02	1.5
9	10	5	40	250	0.04	14.25
10	10	6	20	350	0.06	23.5
11	20	2	30	650	0.04	22.5
12	20	3	35	250	0.06	1
13	20	4	40	350	0.08	10.12
14	20	5	20	450	0.1	3.6
15	20	6	25	550	0.02	6
16	45	2	35	350	0.1	0.5
17	45	3	40	450	0.02	10.5
18	45	4	20	550	0.04	3
19	45	5	25	650	0.06	12.5
20	45	6	30	250	0.08	12.75
21	90	2	40	550	0.06	1.5
22	90	3	20	650	0.08	7.5
23	90	4	25	250	0.1	4.2
24	90	5	30	350	0.02	55.5
25	90	6	35	450	0.04	2.1

Effect of initial sulphate concentration

In order to evaluate the effect of initial sulphate concentration on adsorption process, several solutions were prepared with different concentrations in the range of 250-650 mg/L under optimal conditions. The results in Fig. 5 show that, by increasing the initial sulphate concentration to 350 mg/L, the adsorption rate increased almost linearly. It increased again at lower rate as concentration was increased from 350 mg/L to 650 mg/L.

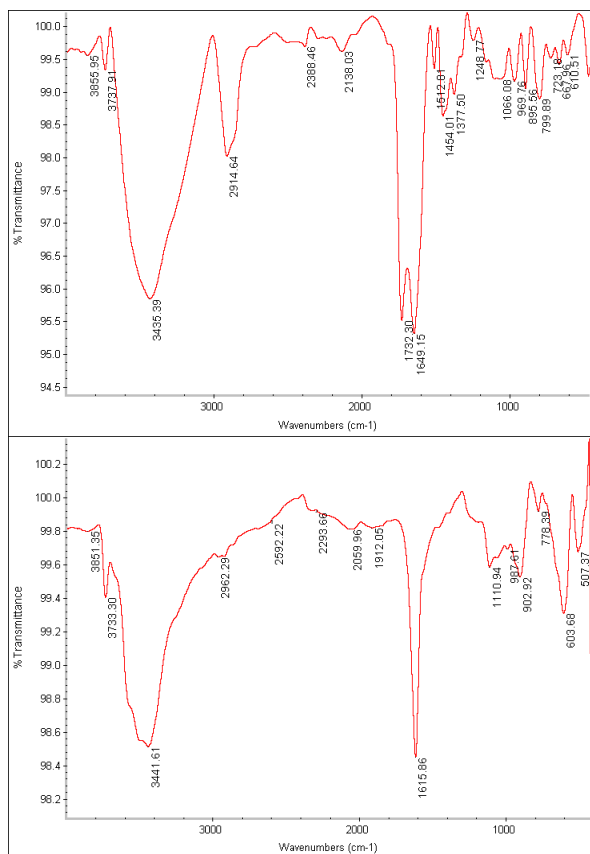


Fig. 2. The FTIR spectrum of raw rice straw (top), and activated carbon mixed with ZnCl₂ (down).

RESULTS AND DISCUSSION

Adsorption isotherm

One of the appropriate tools to model the thermodynamics and kinetics of adsorption process is the use of different methods for determining the adsorption isotherm, which is the relationship between the concentration of adsorbed onto solid surfaces and concentration of contaminants in the liquid phase at equilibrium and constant temperature [14]. The adsorption isotherms are obtained in the laboratory by batch systems [15, 16]. The results obtained from the experimental data are often shown using Langmuir, Freundlich, and Temkin adsorption isotherm models [17,18].

Langmuir isotherm

Langmuir model suggests a monolayer adsorption with no lateral interaction between the adsorbed molecules [19, 20]. This model can be expressed as follows:

$$\frac{C_e}{q_e} = \frac{1}{Q_{max} b} + \frac{C_e}{Q_{max}}, \quad (2)$$

where C_e is the equilibrium concentration of sulphate in solution (mg/L). Q_{max} represents the theoretical monolayer adsorption capacity (mg/g) and b denotes the energy of adsorption (L/mg).

Fig. 6 shows the linearised Langmuir isotherm and the adsorption isotherm parameters are presented in Table 2.

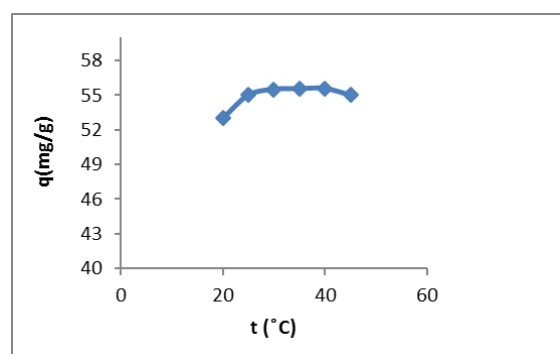


Fig. 3. The effect of temperature on sulfate adsorption (adsorbent dose = 0.02 gr , pH = 5, stirring intensity =200 rpm, sulfate concentration= 350 mg/L and contact time = 90 min).

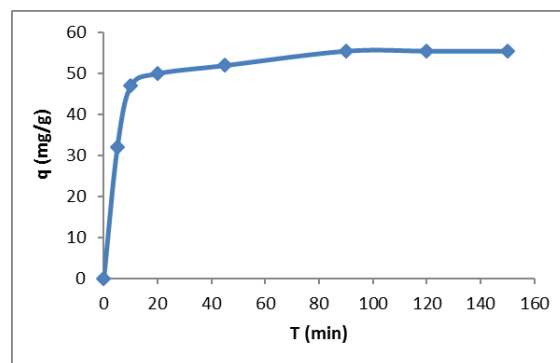


Fig. 4. The effect of contact time on sulphate adsorption (adsorbent dose = 0.02 gr, pH = 5, stirring intensity =200 rpm, sulphate concentration= 350 mg/L and temperature = 30 °C).

Freundlich isotherm

Freundlich model assumes a heterogeneous adsorption process due to the diversity of sorption sites or diverse nature of the ions adsorbed, free or hydrolyzed species [21,22]. The Freundlich model is expressed as follows:

$$\log q_e = \log K_f + 1/n \log C_e, \quad (3)$$

where K_f is the Freundlich constant and n expresses adsorption intensity. By plotting $\text{Log } q$ versus $\text{Log } C_e$, Freundlich isotherm parameters (Fig. 7) can be achieved. The results for Freundlich isotherm parameters are given in Table 2.

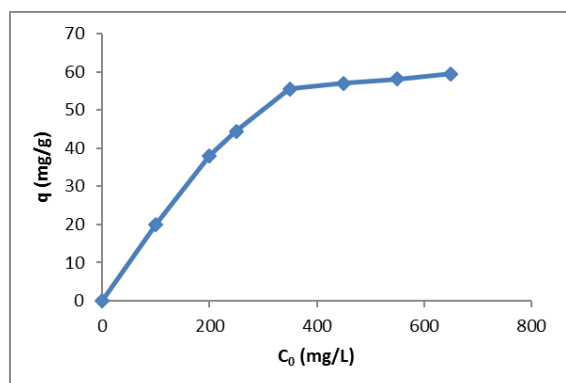


Fig. 5. The effect of initial concentration on sulphate adsorption (adsorbent dose = 0.02 gr , pH = 5, stirring intensity =200 rpm, contact time = 90 min and temperature = 30 ° C).

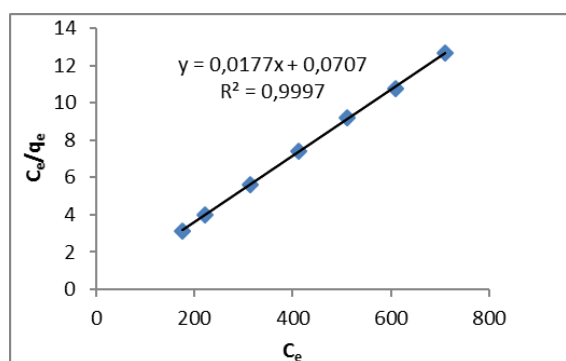


Fig. 6. Linearised Langmuir plot for adsorption of sulphate by activated carbon derived from Rice Straw.

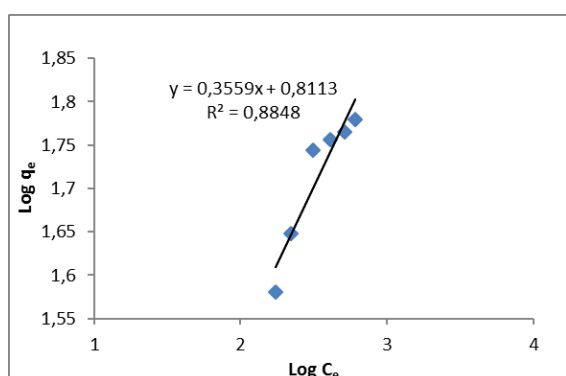


Fig. 7. Linearised Freundlich plot for adsorption of sulphate by activated carbon derived from Rice Straw.

Temkin isotherm

This isotherm contains a factor that explicitly taking into the account of adsorbent-adsorbate interactions. By ignoring the extremely low and large value of concentrations, the model assumes that heat of adsorption (function of temperature) of

all molecules in the layer would decrease linearly rather than logarithmic with coverage. This type of adsorption is expressed as follows:

$$q_e = B \ln A + B \ln C_e, \quad (4)$$

where B is the Temkin constant related to the adsorption heat ($B=RT/b$) and A represents the equilibrium constant hybrid (L/g) that corresponds to the maximum hybrid energy [23,24]. By plotting q versus $\text{Ln } C_e$, the parameters of Temkin isotherm can be calculated (Fig. 8 and Table 2).

As Table 2 shows, the Langmuir equation with a correlation coefficient (R^2) of 0.999 fits well the equilibrium data.

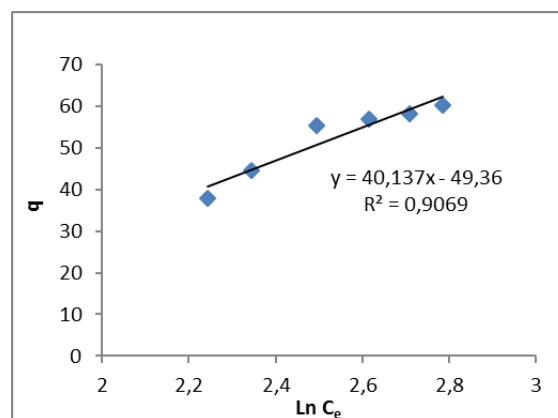


Fig. 8. Linearised Temkin plot for adsorption of sulphate by activated carbon derived from Rice Straw.

Adsorption kinetics

In order to understand the dynamics of adsorption reaction, adsorption kinetics data were studied. It was observed that, with increasing time, the uptake increased. It reached equilibrium state after 90 min of the adsorption process, (Fig. 4). The equilibrium and absorption process depend upon the initial concentration of the absorbed substance. At the early stage (first phase), the adsorption was rapid and, in the second phase, a gradual decline in adsorption can be observed where the diffusion phenomenon was under control. The final phase was the stage of the equilibrium state. Several mathematical models have described the kinetics of adsorption [25]. In this study, first- and second- order kinetics models, inter-particle diffusion kinetics model, and Elovich kinetics model were investigated.

First-order kinetics model

The kinetics data of sulphate were analysed using Lagergren first-order rate equation [26,27,28]:

$$\log(q_e - q_t) = \log q_e - \frac{K_1}{2.303} t, \quad (5)$$

where q_e and q_t are the amounts of sulphate adsorbed (mg/g) at equilibrium and at time t , respectively, and K_1 represents the rate constant of first-order adsorption (1/min). Values of q_e and K_1 are calculated from the slope and intercept of the plot of $\log(q_e - q_t)$ vs t (Fig. 9, Table 3).

Second-order kinetics model

The adsorption kinetics data could be also described by a second-order equation [29,30,31] given below:

$$\frac{t}{q_t} = \frac{1}{K_2 q_e^2} + \frac{1}{q_e} t, \quad (6)$$

where K_2 is the equilibrium rate constant of second-order adsorption (g/mg/min). Values of K_2 and q_e are calculated from the slope and intercept of the plot of t/q vs t (Fig. 10, Table 3).

Inter-particle diffusion kinetics model

This model is based on the diffusion of adsorbed molecules into the adsorption sites within the adsorbent that are available to be checked. The mathematical expression of inter-particle diffusion kinetics model is as follows:

$$q_t = K_p t^{0.5} + C, \quad (7)$$

where K_p is the inter-particle diffusion rate constant ((mg/g).min^{-0.5}) and C denotes inter-particle diffusion constant (mg/g) [32]. Constant values of inter particle diffusion kinetics model are calculated from plot of q_t versus $t^{0.5}$ (Fig. 11, Table 3).

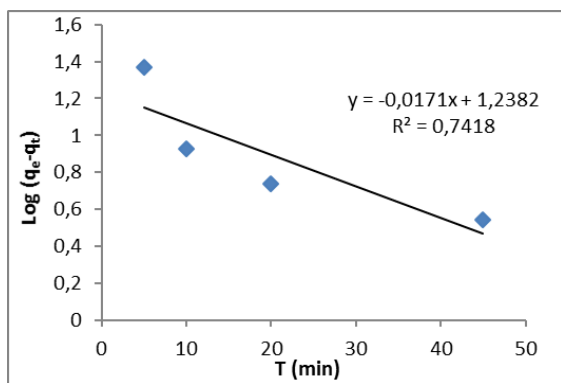


Fig. 9. Plot of the first-order kinetics model for adsorption of sulphate.

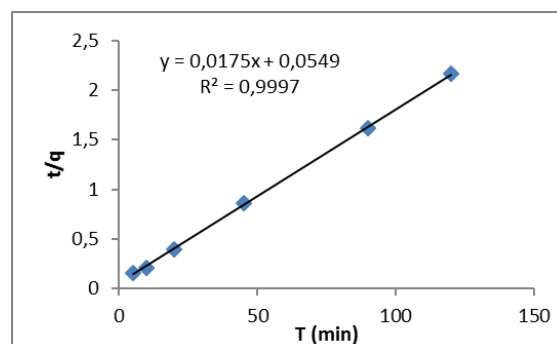


Fig. 10. Plot of the second-order kinetics model for adsorption of sulphate.

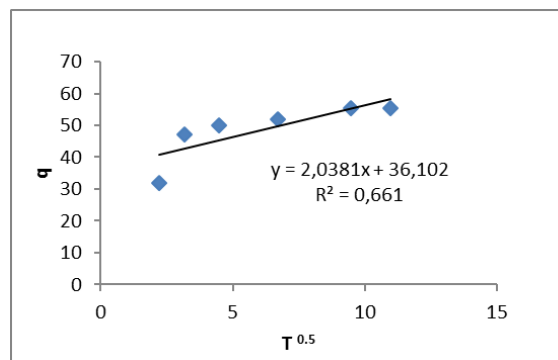


Fig. 11. Plot of the inter particle diffusion kinetics model for adsorption of sulphate.

Elovich kinetics model

The Elovich kinetics equation describes the adsorption and desorption kinetics of minerals used in solid chemistry and can be expressed as follows [32]:

$$q = \left(\frac{1}{\beta}\right) \ln(\alpha\beta) + \left(\frac{1}{\beta}\right) \ln t, \quad (8)$$

where α and β are Elovich constants which are calculated from the plot of q versus $\ln t$ (Fig. 12, Table 3).

As shown in Table 3, based on the analysis of kinetics data on the adsorption process, correlation coefficient was higher for the second-order kinetics model than the other models. This describes that the second-order kinetics model suits well the equilibrium data related to sulphate adsorption by the adsorbent used in this study.

Table 2. Parameters of various isotherm models for sulphate adsorption by activated carbon derived from rice straw.

Langmuir Parameters			Freundlich Parameters			Temkin Parameters		
R ²	q _{max}	b	R ²	k _f	n	R ²	A	B
0.999	56.49	0.25	0.884	6.475	2.81	0.906	3.42	40.14

Table 3. Values of sulphate adsorption kinetics parameters of various models used in this study.

Kinetics models	Parameters		
First-order kinetic	K_1 0.039	q_e 1.23	R^2 0.741
Second-order kinetic	K_1 0.00591	q_e 57.1	R^2 0.999
Inter-particle diffusion kinetic		K_p 2.038	R^2 0.661
Elovich kinetic	α 6.4	β 0.158	R^2 0.806

Table 4. Thermodynamic parameters for the adsorption of sulphate on activated carbon.

ΔG (kJ/mol)						ΔH (kJ/mol)	ΔS (kJ/mol)
T (°C)							
20	25	30	35	40	45	0.001076	10.95
-3.208	-3.230	-3.317	-3.372	-3.427	-3.482		

Thermodynamic studies of adsorption

The relationship between the distribution coefficient (K_d) and temperature in the form of Vant Hoff equation can be expressed as:

$$\ln K_d = \frac{\Delta S}{R} - \frac{\Delta H}{RT} \tag{9}$$

where ΔH is the enthalpy change (kJ/mol), ΔS stands for the entropy change (J/mol.K), R denotes gas constant, and T represents the temperature in Kelvin. The values of ΔH and ΔS are calculated from the slope and intercept of linear regression of $\ln K_d$ versus $1/T$.

The Gibbs free energy change (ΔG) values (kJ/mol) are calculated from the following equation [33-36]:

$$\Delta G = \Delta H - T\Delta S \tag{10}$$

Fig. 13 shows a Linearized plot of Eq. 9 and Table 4 gives the values of thermodynamic parameters. It was found that, the nature of the adsorption reaction is spontaneous and endothermic and the reaction tends to increase the irregularities.

Using EDS and applying SEM analysis the chemical components of the adsorbent were analysed after adsorption process. Results of the interactions of electron beam and activated carbon, plot of the distribution of different chemical elements in the adsorbent and measurement of the percentage of the elements are shown in Figs.14 and 15. In addition, Fig. 16 demonstrates the FTIR spectrum of activated carbon after the adsorption process.

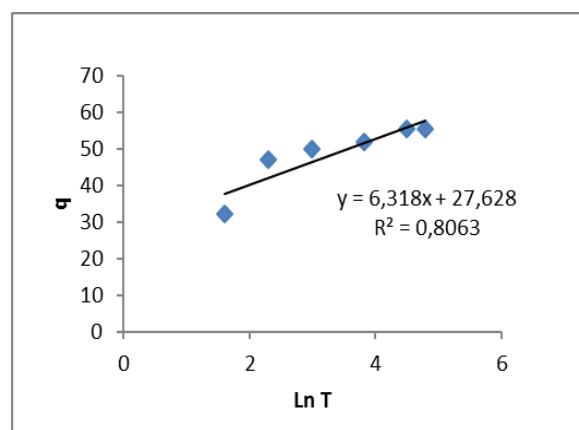


Fig. 12. Plot of the Elovich kinetics model for adsorption of sulphate.

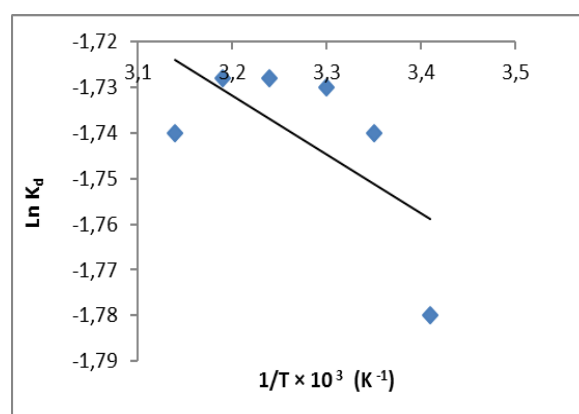


Fig. 13. Plot of $\ln K_d$ vs. $1/T$ for sulphate adsorption on activated carbon.

Distribution of the chemical elements in the adsorbent is presented in Table 5.

Table 5. Distribution of chemical elements in the adsorbent obtained by EDS.

Element. (c/s)	Line 2-sig	Intensity	Weight	Concentration (wt. %)
Si	Ka	6.32	1.005	34.243
S	Ka	0.71	0.338	3.690
Cl	Ka	0.61	0.311	3.078
Zn	Ka	2.55	0.639	58.989
Total				100

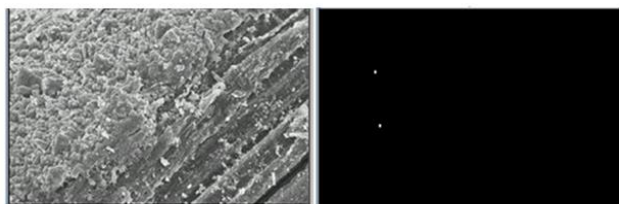


Fig. 14. The image of activated carbon after sulphate adsorption by EDS.

Comparison of ZnCl₂ activated rice straw carbon with other adsorbents

The application of low-cost and easily available materials in wastewater treatment has been widely investigated during recent years. Particularly, the sulphate adsorption on different materials has been extensively studied during recent years. Similar results were also observed for sulphate adsorption using other adsorbents. To illustrate the potential in the use of ZnCl₂ activated rice straw carbon in real applications, a comparative evaluation of the adsorption capacities of various types of adsorbents for the adsorption of sulphate species is provided in Table 6. The results achieved in comparison with the results obtained by others are significant, and so studied adsorbent in sulphate adsorption can be important, in this regard carry out a series of complementary experiments on other characteristics including desorption needs to be done.

Table 6. Adsorption capacity (q) of various adsorbents reported in literature.

Adsorbent	pH	q (mg/g)	Reference
γ-Al ₂ O ₃	5.7	7.7	[38]
Chitin-based shrimp shells	4.5	156	[39]
Powdered TiO ₂	1	0.9	[40]
Soil	4.1	1.42	[41]
Volcanic Ash	4	0.14 (m mol/g)	[42]
Soil	6.2	2.06	[43]
Granite Sand	6.2	1.2	[44]
Coir Pith Carbon	4	0.06	[45]
ZnCl ₂ Activated Coir Pith Carbon	4	4.9	[19]
Magnetite	4	15.4	[46]
LDH (nano particles)	Acidic	30.22	[47]
Rice Straw	Acidic	74.76	[48]
Raw Date Palm Seeds	3.5	3.19	[13]
LDH (nano particles)	7	21 (Percent removal)	[49]
Soil	6.3	0.003	[50]
Poly(m-Phenyl enediamine)	1.75	108.5	[51]
LDH (nano particles)	7	0.13 (m mol/g)	[52]
AMX Membrane	Acidic	80	[53]
ZnCl ₂ Activated Rice Straw Carbon	5	56.49	Present study

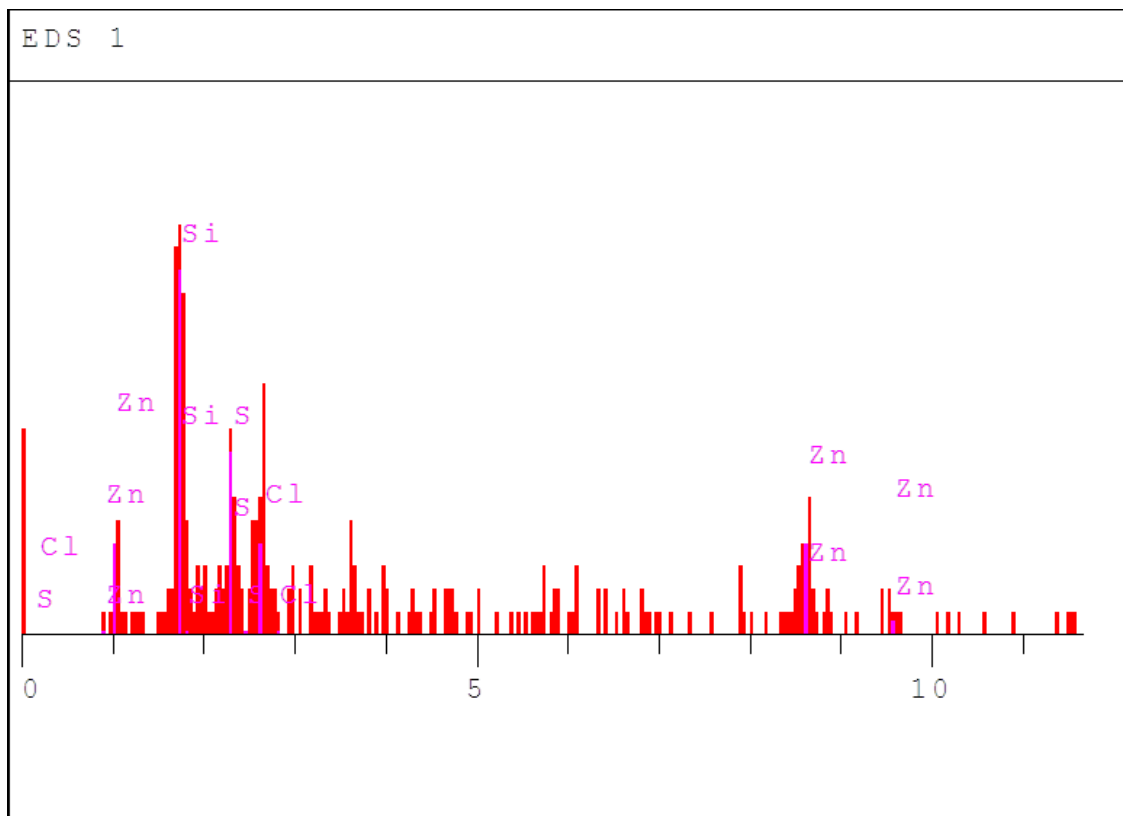


Fig. 15. Distribution of various chemical elements in activated carbon.

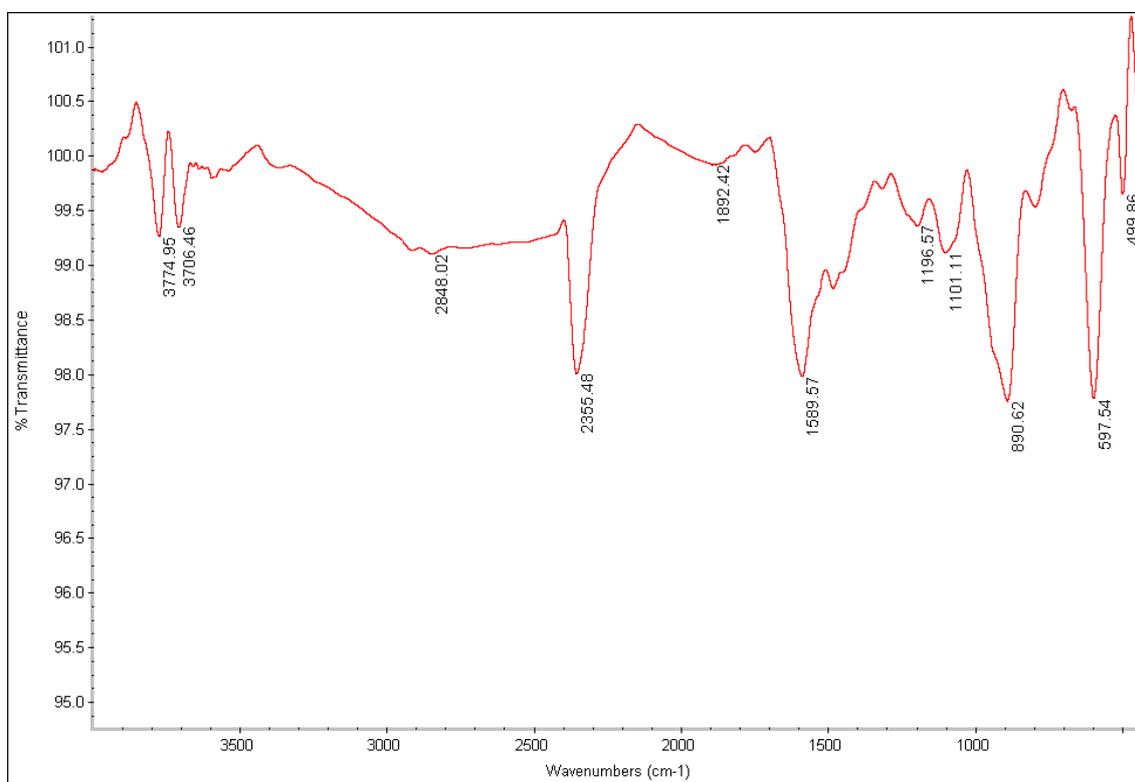


Fig. 16. The FTIR spectrum of activated carbon after adsorption process.

CONCLUSIONS

This study shows that the activated carbon obtained from rice straw and ZnCl₂ boiling solution is an effective absorbent for the removal of sulphate from aqueous solutions. The adsorption equilibrium data was followed by Langmuir isotherm and a second-order model describes the kinetics of process. The maximum absorption capacity was 56.49 mg/g at pH =5, contact time of 90 min, temperature of 30°C, sulphate concentration of 350 ppm, and adsorbent dose of 0.02 gr. Adsorption rate slowly increased with increasing temperature. The adsorption rate was directly proportional to the initial concentration and contact time. The positive values of ΔH^0 , and the negative values ΔG^0 confirmed the endothermic and spontaneous nature of adsorption, respectively.

REFERENCES

1. R.A. Anthony, C.A. Philip, C.J. Peter, S. Leone, N. Daniel, R. Warwick, V. Nafty, *J. Polyhedron.*, **26**, 3479 (2007).
2. G. Sangita, *IJEP*, **30**(11), 953 (2010).
3. A. Maleki, M.B.K. Erfan, A. Mohammadi, R. Ebrahim, *Pakistan J. Biol. Sci.*, **10**, 2348 (2007).
4. A. Maleki, A.H. Mahvi, R. Rezaee, *Sci. J. Kurdistan*, **16**, 65 (2011).
5. S. Lameiras, C. Quintelas, T. Tavares, *Biores. Technol.*, **99**, 801 (2008).
6. A. Maleki, M.A. Zarasvand, *Southeast Asian J. Tropical Medicine & Public Health*, **39**, 335 (2008).
7. C. Quintelas, B. Fonseca, B. Silva, H. Figueiredo, T. Tavares, *Biores. Technol.*, **100**, 220 (2009).
8. D. Sud, G. Mahajan, M.P. Kaur, *Biores. Technol.*, **99**, 6017 (2008).
9. J. M. Dias, M.C.M. Alvim-Ferraz, *J. Environ. Management*, **85**, 833 (2007).
10. A.A. Nunes, A. S. Franca, *Biores. Technol.*, **100**, 1786 (2009).
11. A. Ahmadpour, D.D. Do, *Carbon*, **35**, 1723 (1997).
12. C.F. Liu, F. Xu, J.X. Sun, J.L. Ren, S. Curling, R.C. Sun, *Carbohydrate Res.*, **341**(16), 2677 (2006).
13. S. Koumaiti, K. Riahi, F. Ounaies., B. Thayer, *J. Environ. Sci. Eng.*, **5**, 1570 (2011).
14. K.M. Khoda, Adsorption Isotherms, Nanyang: Nanyang Technological University, 2009.
15. B.H. Hameed, *J. Hazard. Mater.*, **162**, 939 (2009).
16. F. D.Ardejani, K. Badii, N.Y. Limaee, S. Shafaei, A. Mirhabibi, *J. Hazard. Mater.*, **151**, 730 (2008).
17. I. Langmuir, *J. Am. Chem. Soc.*, **40**, 1361 (1918).
18. H. Freundlich, *Z. Phys. Chem.*, **57**, 387 (1906).
19. C. Namasivayam, D. Sangeetha, *Desalination*, **219**, 1 (2008).
20. A.E. Nemr, *J. Hazard. Mater.*, **161**, 132 (2009).
21. B. Subramanyam, A. Das, *Int. J. Environ. Sci. & Technol.*, **6**, 633 (2009).
22. O. Altin, O. Ho, T. Dogu, *J. Colloid Interface Sci.*, **198**, 130 (1998).
23. S. Lagergren, *Hand Linger*, **24**, 1 (1898).
24. M. Temkin, J.A.V. Pyzhev, *Acta Physiochem.*, **12**, (1940) 217.
25. G.S. Khorramabadi, R.D.C. Soltani, S. Jorfi, *J. Water & Wastewater*, **1**, 57 (2010).
26. H. Qiu, L. Lv, B.C. Pan, Q. Zhang, W. Zhang, Q. Zhang, *J. Zhejiang Univ. Science A*, **10**(5), 716 (2009).
27. X. Fan, D.J. Parker, M.D. Smith, *Water Res.*, **37**, 4929 (2003).
28. S Lagergren, *PA Norstedt & Söner*, **24**, 1 (1898).
29. Y. Ho, *J. Hazard. Mater.*, **136**, 103 (2006).
30. Y.S. Ho, G. McKay, *Chem. Eng. J.*, **70**, 115 (1998).
31. W. Enos, K.M. Gerald, M. Paul, J. Karanja, *Eurasian J. Sci. Res.*, **4**, 317 (2009).
32. J. Wu, H.Q. Yu, *Biores. Technol.*, **98**, 253 (2007).
33. D.L. Sparks, in: Soil Physical Chemistry, CRC Press LLC, 1999, 38.
34. M. Torab-Mostaedi, *Chem. Ind. & Chem. Engineering Quart.*, **19**, 79 (2013).
35. S.J. Malakooti, S.Z.S. Tonkaboni, M. Noaparast, F.D. Ardejani, R. Naseh, *Environ. Earth Sci.*, **71**, 2267 (2014).
36. A. Halajnia, S. Oustan, N. Najafi, A.R. Khataee, A. Lakzian, *Appl. Clay Sci.*, **80-81**, 305 (2013).
37. A. Kumar, V. Kumar, *J. Chem. Pharm. Res.*, **7**, 685 (2015).
38. C.H. Wu, C.Y. Kuo, C.F. Lin, S.L. Lo, *Chemosphere*, **47**, 283 (2002).
39. A. Moret, J. Rubio, *Minerals Eng.*, **16**, 715 (2003).
40. G. Horanyi, *J. Colloid Interface Sci.*, **261**, 580 (2003).
41. M.E. Alves, A. Larorenti, *Geoderma*, **118**, 89 (2004).
42. T. Delfosse, P. Delmelle, B. Delvaux, *Geoderma*, **136**, 716 (2006).
43. V.E. Osodeke, A.F. Ubah, *Agric. J.I.*, **2**, 48 (2006).
44. M.N. Khan, U. Zareen, *J. Hazard. Mater. B*, **133**, 269 (2006).
45. C. Namasivayam, *J. Environ. Eng. Management*, **17**, 129 (2007).
46. P. Roonasi, A. Holmgren, *J. Colloid Interface Sci.*, **333**, 27 (2009).
47. K. Khalatbari, E. Jorjani, S. Bazgir, Study Sulfate Adsorption of Copper Sulfate Using LDH nano particles, Department of Technology, Science and Research Branch, Islamic Azad University, Tehran, Iran, 2010, p. 1.
48. W. Cao, Z. Dang, X.Q. Zhou, X.Y. Yi, P.X. Wu, N.W. Zhu, and G.N. Lu, *Carbohydrate Polym.*, **85**, 571 (2011).
49. U. Rafique., A Imtiaz, A.K. Khan, *J. Water Sustain.*, **2**, 233 (2012).
50. G. K. Ghosh, N. R. Dash, *Animal & Environ. Sci.*, **2**, 2231 (2012).
51. P.L. Sang, Y.Y. Wang, L.Y. Zhang, L.Y. Chai, and H.Y. Wang, *Trans. Nonferrous Metals Soc. China*, **23**, 243 (2013).
52. A. Halajnia, S. Oustan, N. Najafi, A.R. Khataee, A. Lakzian, *Appl. Clay Sci.*, **80-81**, 305 (2013).
53. Ch. Hannachi, F. Guesmi, Kh. Missaoui, *Int. J. Technol.*, **5**, 60 (2014).